POAC'17
Busan, KOREA

Proceedings of the 24th International Conference on
Port and Ocean Engineering under Arctic Conditions
June 11-16, 2017, Busan, Korea

Sensor Arrangement for Ice Load Monitoring to Estimate Local Ice Load in Arctic Vessel

Young-Chun Jo[1], Joong-Hyo Choi[1], Sung-Gun Park[1], Sungkon Han[1]
[1] Ship & Ocean R&D Institute (Daewoo Shipbuilding & Marine Engineering, Seoul, Korea)

ABSTRACT

The more opportunities for exploitation and transportation are given in the Arctic area, the larger commercial vessels are needed for mass transportation. The environmental loads due to the interaction between ice and hull are increased to enlargement of arctic vessels. The ice load monitoring system is recommended for the research of ice load estimation and the safety of hull structure. This paper is concerned with sensors arrangement for ice load monitoring in arctic vessel. The number and arrangement of sensors were determined for the estimation of ice induced loads acting on the hull. FE analyses were carried out to verify the estimation of ice loads. The alternative arrangement of sensors was proposed considering complex structural details which cause the stress concentrations and discontinuities.

KEY WORDS: Sensor; Sensor arrangement; Ice load; Ice load monitoring; Arctic vessel.

INTRODUCTION

The activities related to exploitation for oil and gas in the Arctic areas increase significantly. In order to transport increased resources in the Arctic areas, large Arctic commercial vessels such as gas carriers, oil tankers, bulk carriers, etc. are needed for mass transportation. In Arctic area, ice is the main factor of environmental load acting on Arctic vessel. The ice load is increased with the enlargement of vessel.

The largest Arctic commercial vessel was built by DSME. Table 1 shows main dimension of Arctic LNG carrier. The size of Arctic LNG carrier is larger than any other Arctic vessels have been constructed so far. Ice load monitoring system was installed for safety of ice navigating and hull structure of this large LNG carrier.

Table 1. Main dimensions of Arctic LNG carrier

	Length (LOA)	Breadth	Height
Dimension(m)	Abt. 300	50	26.5

This paper is concerned with sensors arrangement for ice load monitoring in arctic vessel. The number and arrangement of sensors are determined for the estimation of ice induced loads acting on the hull. FE analyses were carried out to verify the estimation of ice loads. The alternative arrangement of sensors was proposed considering complex structural details which cause the stress concentrations and discontinuities.

ICE LOAD MONITORING SYSTEM (ILM)

Ice load monitoring system consists of sensors, wire, data acquisition device, data process device and so on. Because sensors are installed directly on the structure at measuring location and ice load on hull structure is estimated based on measured electrical signal of these sensors, the number and arrangement of them are crucial in ILM.

Installed Locations of Sensors

The installed locations of strain sensors were determined considering expected high ice loaded area. Figure 1 shows the sensors installed locations for ILM.

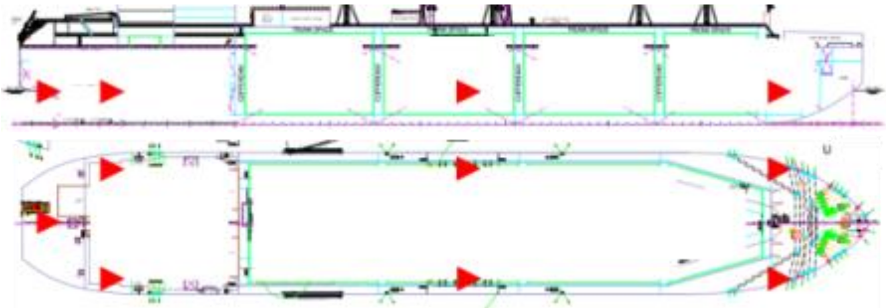

Figure 1. Sensors installed locations for ILM

Sensors Arrangement

The arrangement of strain sensors at each location is shown as figure2. The type and purpose of arranged sensors are described as follows.

- The sensors on flange of longitudinal/transverse frame have 1-axis filament. They measure bending stress of frame.
- The sensors on both web ends of longitudinal/transverse frame have 2-axis filament.

They measure shear stress of frame.

- The sensors on side shell have 3-axis filament. They assess the damage of hull plate.

Finally, 49 strain gauges were installed in Arctic LNG carrier.

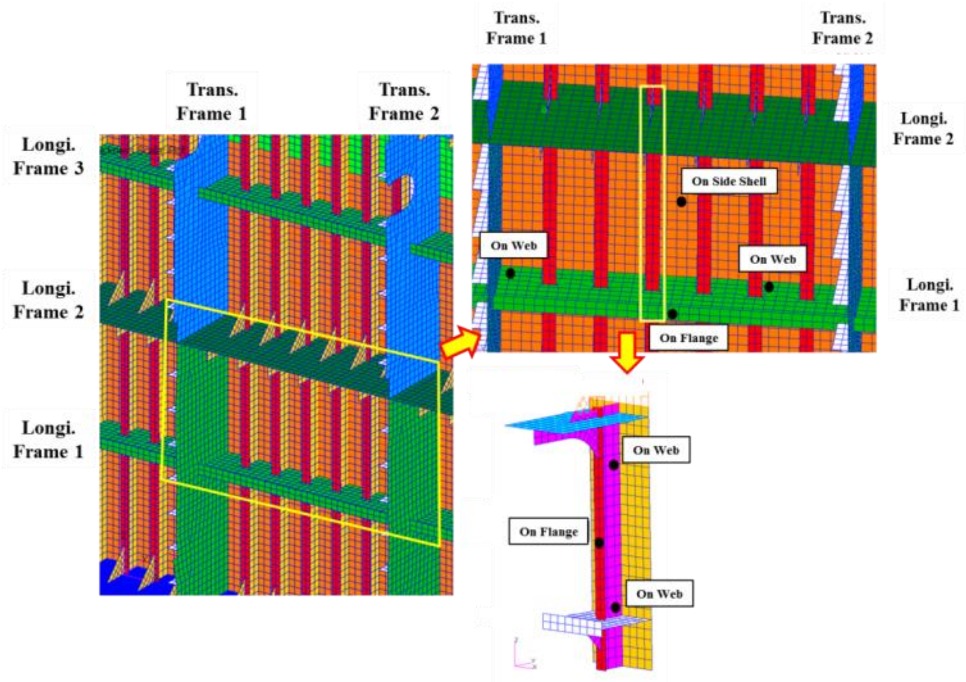

Figure 2. Details of Sensors Arrangement in Measuring Area

ICE LOAD ESTIMATION

In this section, the procedure of stress calculation from measured strain value at sensors and estimation of ice load which is derived from stress components were described.

Calculation of Stress Components

The stress in the cross section of the stiffener was divided into axial, transverse and shear stress. Eq. (1) is the general expression for principal strain directions at any location.

$$\varepsilon(\phi) = \frac{\varepsilon_x + \varepsilon_y}{2} + \frac{\varepsilon_x - \varepsilon_y}{2} \cdot \cos(2\phi) + \frac{1}{2} \cdot \gamma_{xy} \sin(2\phi) \qquad (1)$$

Where, ϕ is the degree of angle about x-axis with 2 dimensional Cartesian coordinate system.

Because the strain sensor with 3-axis filament can measure 3 principal strain directions, stress components can be obtained by stress-strain relation. But, the study result proposed by Holm (2012) was applied to prevent increase of the number of sensor. Holm (2012) showed that the strain sensor with 2-axis filament can calculate the stress components in a particular case.

The strain sensors with 2-axis filament were installed near the both ends of stiffener avoiding bracket as shown in Figure 3. The sensors were located on neutral axis.

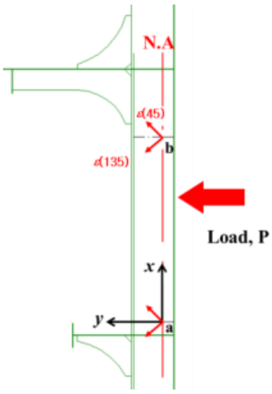

Figure 3. Sensors Arrangement of Frame

X axis is parallel with length direction of stiffener. The filaments of each strain sensor were attached at angles of 45 degrees and 135 degrees, respectively.

Eq. (2) is the matrix form of Eq. (1) considering angles of filament arrangement. $\varepsilon(0)$ is assumed as the dummy strain.

$$\begin{bmatrix} \varepsilon(0) \\ \varepsilon(45) \\ \varepsilon(135) \end{bmatrix} = \begin{bmatrix} 1 & 0 & 0 \\ \frac{1}{2} & \frac{1}{2} & \frac{1}{2} \\ \frac{1}{2} & \frac{1}{2} & -\frac{1}{2} \end{bmatrix} \cdot \begin{bmatrix} \varepsilon_x \\ \varepsilon_y \\ \gamma_{xy} \end{bmatrix} \tag{2}$$

By solving Eq. (2), the strain components of Cartesian coordinate is obtained as Eq. (3)

$$\begin{bmatrix} \varepsilon_x \\ \varepsilon_y \\ \gamma_{xy} \end{bmatrix} = \begin{bmatrix} 1 & 0 & 0 \\ -1 & 1 & 1 \\ 0 & 1 & -1 \end{bmatrix} \cdot \begin{bmatrix} \varepsilon(0) \\ \varepsilon(45) \\ \varepsilon(135) \end{bmatrix} \tag{3}$$

On beam bending problem, the axial strain along neutral axis is 0 (zero).

$$\varepsilon_x = 0 \tag{4}$$

Strain components can be obtained from measured strain $\varepsilon(45)$, $\varepsilon(135)$ using Eq. (3).

$$\varepsilon_y = \varepsilon(45) + \varepsilon(135), \quad \gamma_{xy} = \varepsilon(45) - \varepsilon(135) \tag{5}$$

Stress components can be calculated as stress-strain relation.

$$\sigma_x = E\varepsilon_x = 0, \quad \sigma_y = E\varepsilon_y, \quad \tau_{xy} = G\gamma_{xy} \tag{6}$$

Load Estimation

When load P_{app} is applied between sensor positions, shear stresses at each gauge are respectively obtained as τ_a and τ_b according to the previous section as Figure 4.

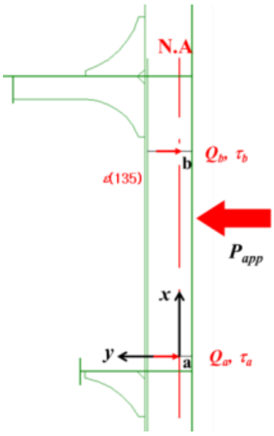

Figure 4. Frame acting on applied load, P_{app}

Estimated load, P_{est}, can be derived from shear forces at the sensor positions.

$$P_{est} = Q_a - Q_b = f_Q \cdot (\tau_a - \tau_b) \cdot A_w \tag{7}$$

Where, f_Q is the correction factor and A_w is the cross-sectional area of web.

For accuracy of estimation, estimated load should be same as applied load. If applied load, P_{app}, is known and shear stresses can be calculated by FEA, correction factor f_Q can be obtained as Eq. (8).

$$f_Q = \frac{P_{app}}{(\tau_a - \tau_b) \cdot A_w} \tag{8}$$

FE ANALYSIS

FE analysis was carried out in order to verify the arrangement of strain sensors. MSC PATRAN/NASTRAN was used for FE analysis.

FE Models

While the number of sensors installed locations was seven (7), the number of models was reduced to four (4) considering symmetry. Figure 5 shows FE models and detail in each sensor installed location. Very fine mesh for more detailed distribution of stress components was used in the models. Figure 6 shows very fine meshed details of transverse and longitudinal frames in fore body model.

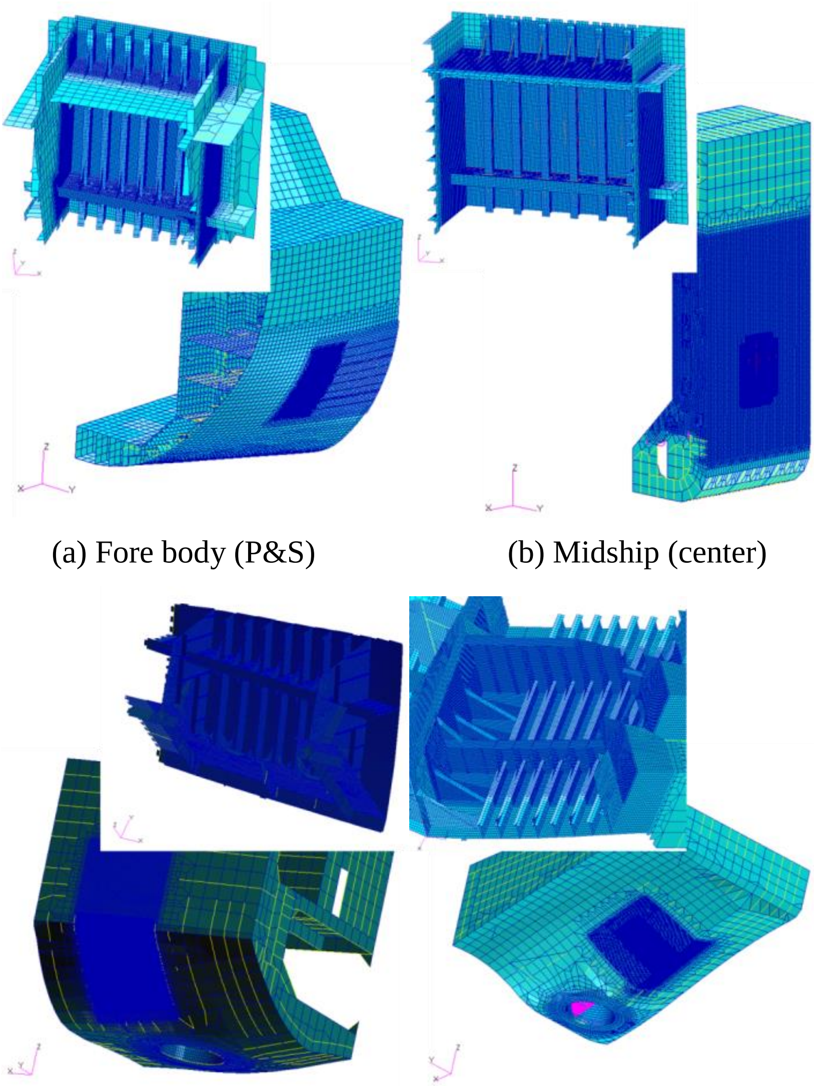

(a) Fore body (P&S) (b) Midship (center)

(c) Aft. body (P&S) (d) Aft. body (center)

Figure 5. FE Models and Detail of measured area

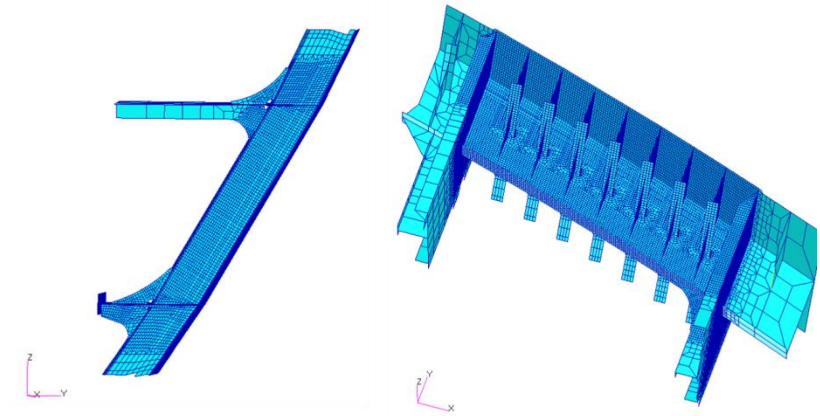

(a) transverse frame (b) longitudinal frame

Figure 6. Details of Frames (fore body)

Loading & BCs

It was assumed that relationship between applied load and structural response is linear. Unit load (1kN) was applied to FE model. Area subject to ice load was determined considering ice navigating draft of Arctic LNG carrier. In order to consider the vessel's movement, 17 load steps were created as Figure 7.

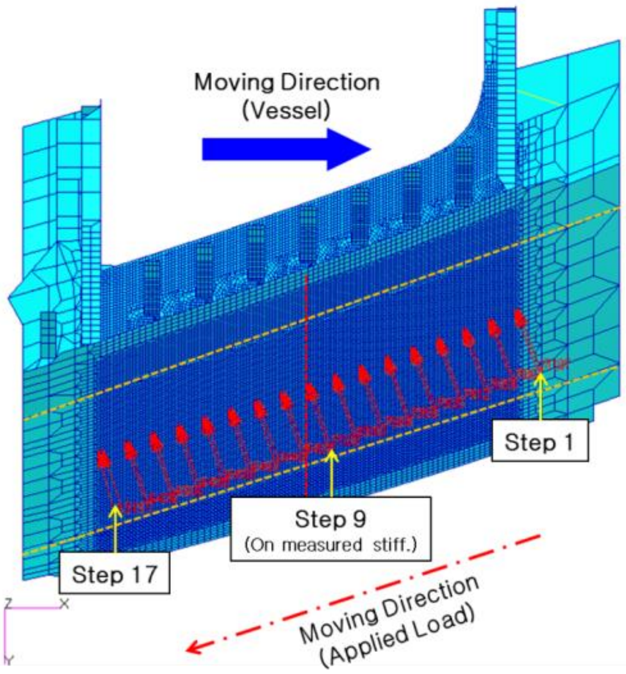

Figure 7. Scheme of Load Step

Results

Figure8 shows shear stress distribution in transverse frame and the graph of shear stress distribution on neutral axis. Load estimation results of transverse frame were shown in Table 2.

Table 2. Load Estimation Result of Transverse Frame

Position	Shear force (kN)	Est. load (kN) a – b	Applied load (kN)	Correction factor, f_Q
Sensor a	0.517	0.970	1.00	1.03
Sensor b	-0.453			

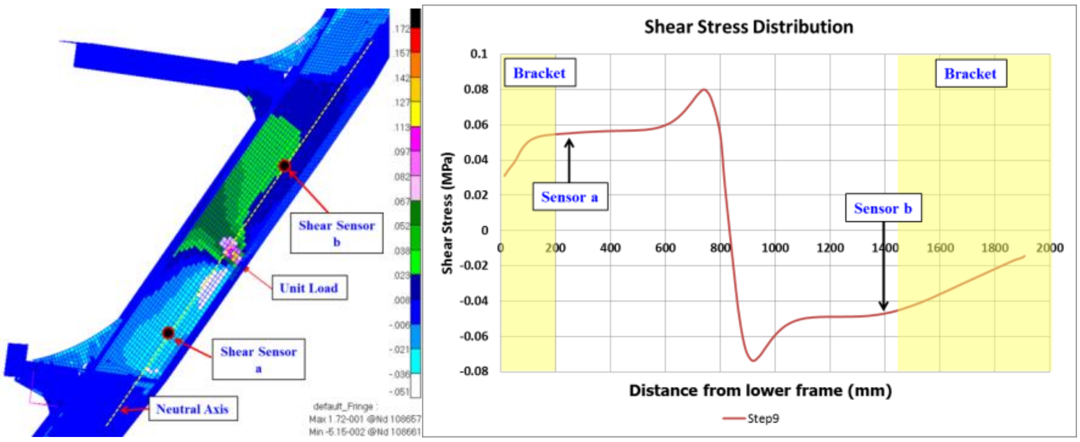

Figure 8. Shear Stress Distribution in Transverse Frame

Figure9 shows shear stress distribution in longitudinal frame and the graph of shear stress distribution on neutral axis. At connections with transvers frames, stress concentrations and discontinuities were shown.

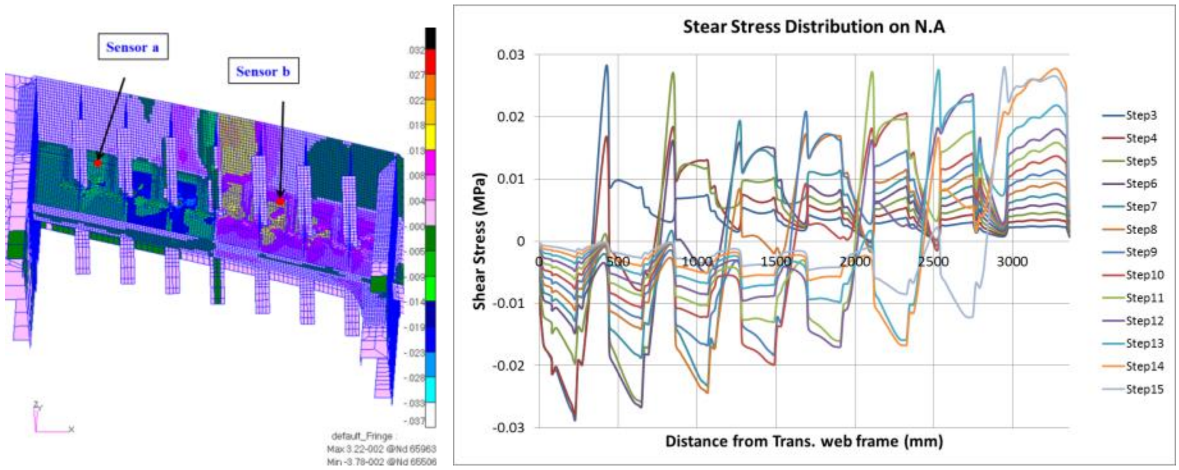

Figure 9. Shear Stress Distribution in Longitudinal Frame

Load estimation result from shear stress at positions of sensors is shown in Figure 10. Estimated values from load step 5 to load step 11 were stable. Correction factor was able to be obtained using average estimated value of stable load steps as table 3. In spite of structural discontinuity, load could be estimated from strain sensors.

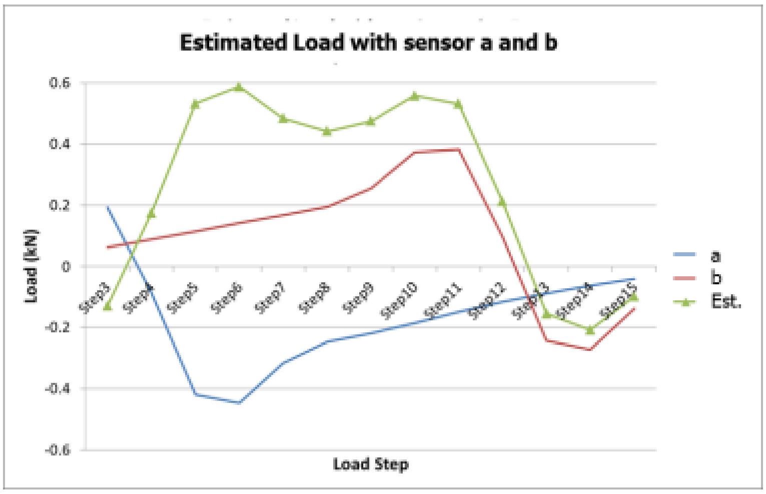

Figure 10. Estimated Load at Load Steps

Table 3. Load Estimation Result of Longitudinal Frame

Position	Avg. Est. load (kN)	Applied load (kN)	Correction factor, f_Q
Sensor a	0.516	1.00	1.94
Sensor b			

Modification of Sensors Arrangement

In longitudinal frame, strain sensors were not able to be installed because the residual area considering transverse frame connections, such as slot hole and collar plate, is smaller than the required area for sensors installation. Positions of strain sensors in longitudinal frame were modified out of neutral axis. Shear stress distribution on cross-sectional area at each sensor's position was reviewed above all as Figure 11. Although stress at upper part of cross-section was smaller than lower part, distribution trends were similar with each other. Load estimation with strain sensors out of neutral axis was able to carry out through the recalculation of correction factor.

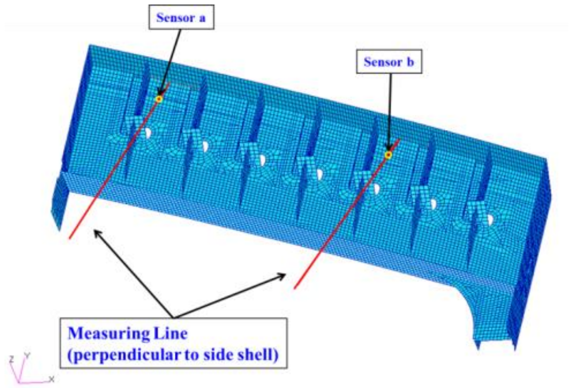

(a) Reviewed Line at Each Sensor's Position

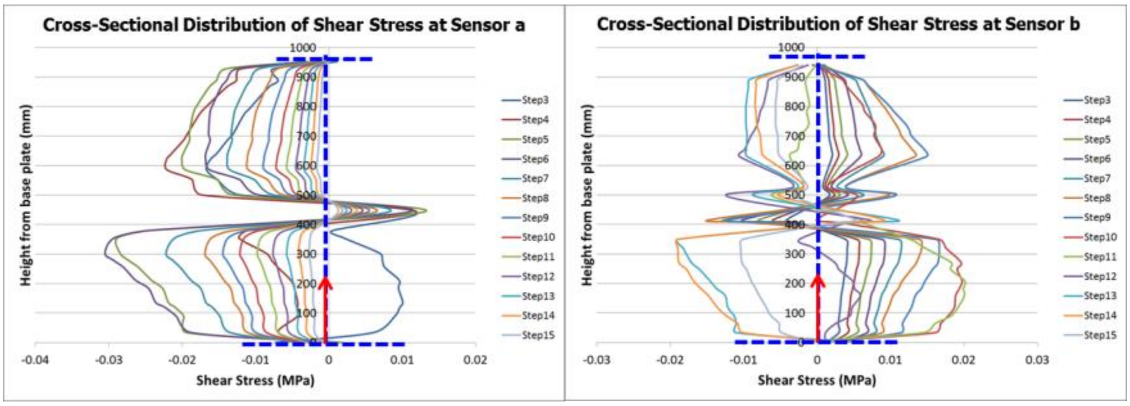

(a) sensor a (b) sensror b

Figure 11. Cross-Sectional Distribution of Shear Stress in Longitudinal Frame

Load estimations were carried out with candidates (a', a'', b') for modified sensors positions as Figure 12. Estimation results are shown in Figure 13. The result with a'' and b' was more stable, alternative positions of strain sensors were determined. Table 4 shows estimation result and correction factor of modified positions.

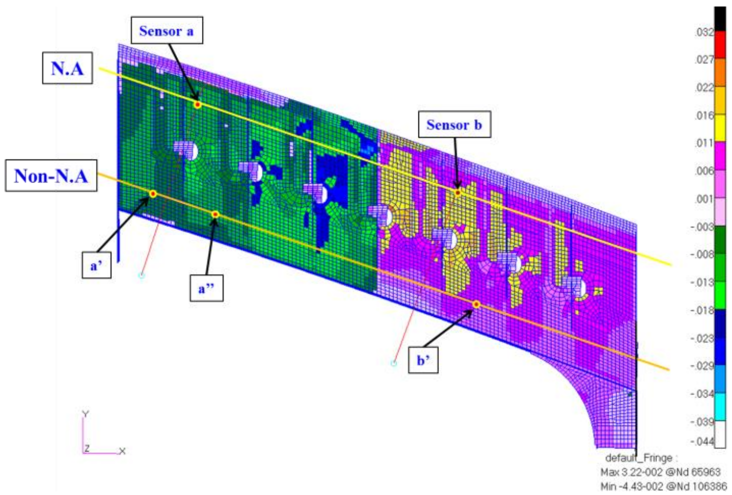

Figure 12. Modified Arrangement of Strain Sensors in Longitudinal Frame

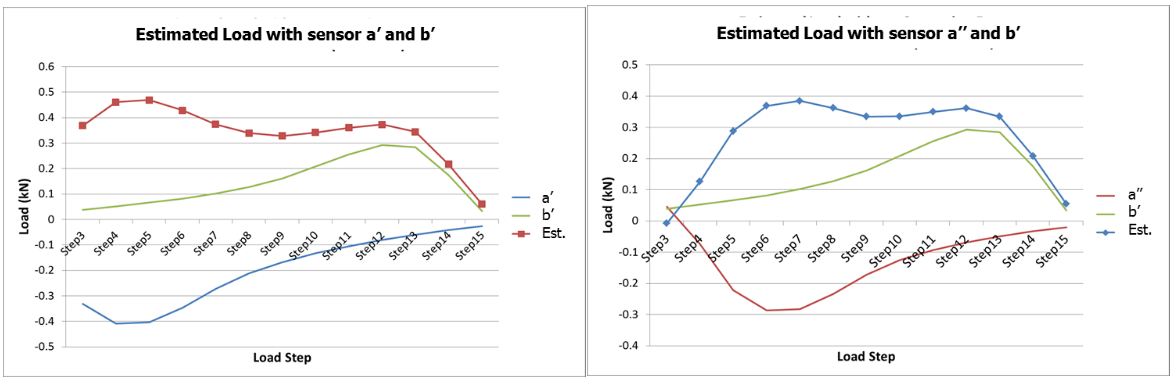

Figure 13. Load Estimation Results

Table 4. Load Estimation Result of Modified Position

Position	Avg. Est. load (kN)	Applied load (kN)	Correction factor, f_Q
Sensor a''	0.356	1.00	2.81
Sensor b'			

CONCLUSIONS

- The seven (7) locations for the installation of strain sensors were determined in Arctic LNG carrier built by DSME. Seven (7) strain sensors are required at each location. Total 49 strain sensors were used for ice load monitoring in Arctic LNG carrier.
- Strain components could be derived from 2-axis strain sensors on neutral axis of longitudinal/transverse frames. Stress component could be obtained with stress-strain relationship and load estimation could be performed.
- FE analyses were carried out in order to verify sensors arrangement and load estimation. Load could be estimated with proposed sensors arrangement despite structural discontinuity and stress concentration of complex stiffened structure.
- Sensors in longitudinal frame were moved out of neutral axis due to installation problem. Load estimation could be carried out.

ACKNOWLEDGEMENTS

This work was supported by the Industrial Convergence Strategic technology development program (10063417, Development of basic design technology for ARC7 class Arctic offshore structures) funded by the Ministry of Trade, industry & Energy (MI, Korea).

REFERENCES

Choi, J., Park, G., Kim, Y., Jang, K. Park, S., Ha, M., Yu, H., Iyerusalimskiy, A. & St. John, J., 2009. Ice Load Monitoring System for Large Arctic Shuttle Tanker, Proceedings of International Conference on Ship and Offshore Technology,

Holm, H., 2012. *Ice-Induced Loads on Ship Hulls*. Master Thesis: Norwegian University of Science and Technology.

Iyerusalimskiy, A., Choi, J., Park, G., Kim, Y. & Yu, H., 2011. The Interim Results of the Long-term Ice Loads Monitoring on the Large Arctic Tanker, *Proceedings of the 21st International Conference on Port and Ocean Engineering under Arctic Conditions*, paper No. POAC11-088

Leira, B., Børsheim, L., Espeland, Ø. & Amdahl, J., 2009. Ice-Load Estimation for a Ship Hull based on Continuous Response Monitoring, *Proceedings of the Institution of Mechanical Engineers*, Vol. 223 pp.529-540.

Yu, H., Iyerusalimskiy, A., Kim, Y. S. & St. John, J., 2012. Hull Structural Performance Monitoring System for Ships Operating in Ice-Covered Waters, *Proceedings of the Arctic Technology Conference*, paper No. 1368063.